J Supercond Nov Magn (2013) 26:1319–1324
DOI 10.1007/s10948-012-1857-x

ORIGINAL PAPER

Isotope Effect at the Fano Resonance in Superconducting Gaps for Multiband Superconductors at a 2.5 Lifshitz Transition

Davide Innocenti · Antonio Bianconi

Received: 8 November 2012 / Accepted: 30 November 2012 / Published online: 5 January 2013

Abstract The doping dependent isotope effect in cuprates is explained in the framework of shape resonances in the superconducting gaps (belonging to the class of Fano resonances) in multicondensate superconductors. This new paradigm for high temperature superconductivity is based on the recent Fermiology scenario emerging from dHvA and quantum oscillation data showing a 2.5 Lifshitz topological transition due to the appearance of new small Fermi surface in the underdoped regime. The isotope effect is calculated for an electronic system near a band edge for a superlattice of stripes. The model reproduces the doping dependence of the isotope exponent behavior in cuprates and allows to identify the relative role of the intraband Cooper pairing and the configuration interaction between pairing channels from experimental data.

Keywords Multi-condensate superconductors · Shape resonance · Fano resonance · Lifshitz transition · Isotope effect

1 Introduction

There is growing compelling evidence for the presence of a 2.5 Lifshitz electronic topological transitions in the normal phase of cuprate superconductors changing the doping of the CuO_2 layer [1] following the extended experimental activity in the detection of Fermi surface pockets in cuprate superconductors [2–11]. These results imply the paradigm shift away from the "single band," "single component" dogma for high temperature superconductivity near a Mott insulator. The "single band" dogma, was assumed by the majority of the scientific community for more than 25 years motivated by theoretical arguments against experimental data showing multiple electronic components [12–14], and proposed theories considering a normal metal with multiple bands [15] and multigap multi-condensate superconductivity [16, 17].

The Fermi surface reconstruction can be due to magnetic or charge or lattice modulations. The lattice complexity has been unveiled by experimental probes using synchrotron radiation, Extended X-ray Absorption Fine Structure (EXAFS), and X-ray Absorption Near Edge Structure (XANES) that have been shown to detect structural nanoscale polymorphism with deviation from the average structure like in surfaces [18], layered oxides [19], and liquids [20, 21]. These methods have allowed the identification of short range lattice fluctuations that decorate the CuO_2 plane by lattice stripes [22–27] with ordering of oxygen interstitials [28, 29] and local lattice distortions [30–35].

Different electronic components (ii) polaronic charge carriers compete and coexist with delocalized carriers in a different Fermi surface spots [36, 37]. In this scenario, the high temperature superconductors show a generic complex phase separation [38] with the appearance of superconductivity in a complex network of superconducting striped grains [39, 40].

In order to solve the mechanism for high T_c superconductivity, the interpretation of the anomalous isotope effects [41–46] remains of high interest.

In this paper, we provide a possible interpretation of the anomalous isotope effect as arising from the proximity of the chemical potential to a 2.5 Lifshitz transition in the normal phase considering multi-condensate superconductivity in striped superconducting domains [47–51]. The insulator to superconductor transition (SIT) at hole doping $\delta = 1/16$

D. Innocenti · A. Bianconi (✉)
RICMASS, Rome International Center for Materials Science Superstripes, Via dei Sabelli 119A, 00185 Roma, Italy
e-mail: antonio.bianconi@ricmass.eu

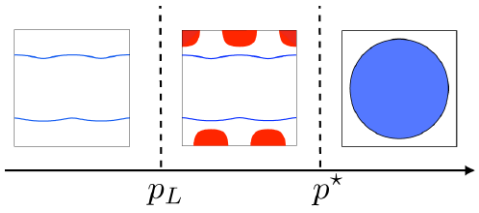

Fig. 1 Doping dependence of the Fermi surface topology in doped Mott insulators: cuprates as deduced by quantum oscillation experimental data Refs. [1, 2] in hole doped cuprates. At the critical hole doping $P_L = 2/16$ there is a 2.5 Lifshitz transition where the reconstructed Fermi surface of the normal phase undergoes a change of topology: the electron like blue lines indicate a open 1D Fermi surfaces, the closed red spots are small electron pockets appearing at P_L. At $p^* \approx 3/16$ the two small Fermi surfaces merges in the large Fermi surface predicted for the undistorted lattice at high doping

occurs with the appearance of Fermi surface spot modeled as a one dimensional band as shown in Fig. 1. The quantum oscillation data [1] show that at doping $P_L = 2/16$ a second electron-like circular Fermi surface (red in color on line) appears. Beyond the second critical doping p*, the large Fermi surface (blue color on line) of the undistorted CuO_2 plane appears.

The appearance of the second electron Fermi surface shown in Fig. 1 is a 2.5 Lifshitz topological transition from a single band to a two-band superconductor with the appearance of a second electron-like closed Fermi surfaces. This 2.5 Lifshitz transition is an electronic topological transition (ETT) for the appearing of a new 2D Fermi surface spot.

Here, we present a simple theoretical model that is able to grab the essential physics of multicomponent superconductivity near a 2.5 Lifshitz transition [37–41]. The model includes the BEC-BCS crossover in a multi condensate superconductor and predicts the doping dependent isotope effect [41, 42].

The experimental determination of the isotope effect on the superconducting critical temperature T_c of simple metals [52, 53] induced by the isotope substitution has been found to follow a power law dependence $T_c \propto M^{-\alpha}$, where M is the atomic mass and α is the isotope coefficient (IC). The exponent $\alpha = 0.5$ in agreement with the prediction of the BCS theory is usually observed in conventional BCS superconductors. This experimental agreement has been considered the definitive proof for the electron-phonon interaction driving the formation of the electron pairs on the Fermi surface.

The IC exponent $\alpha = 0.5$ is correct only for the case of a single band metal with a large Fermi surface, a high Fermi energy, and a constant density of states (DOS) above and below E_F for a harmonic electron-lattice interaction. Most of the isotope measurements in cuprate superconductors have been performed by replacing ^{16}O with ^{18}O [41–44]. The measured change of T_c with isotope substitution of atoms other than oxygen is very small. The dominant isotope effect in the case of $YBa_2Cu_3O_{7-y}$ (Y123) is associated with the planar O's, and this suggests that the planar tilting or buckling modes in the CuO_2 layers determine an important phonon contribution to the effective e–e pairing interaction. Y123 shows at low doping an isotope effect of the order of 0.5 and drops in the range of optimum doping, $T_c = 92$ K, at very small values of α between 0.0 and 0.1 like for the La214 families. These strong deviations of the IC from the standard 0.5 value have been considered the smoking gun for unconventional superconductivity.

Various attempts have been made to explain the peculiar features of the isotope coefficient in cuprate superconductors by taking into account the effects of anharmonicity, temperature dependent strong magnetic pair breaking due to impurities, condensation of charged and interacting local bosons, and structural instability [52, 53].

2 The Model

Considering the phase diagram of cuprate superconductors in the range of the doping smaller than $P_L = 1/8$, the planar metallic layers show a Fermi surface topology made of open lines or arcs as shown in Fig. 1. The physical origin of this one-dimensional (1D) Fermi surface in this doping range is well known as the stripes scenario where the 2D metal is decorated by a striped pattern of lattice, spin, and charge modulations. The Lifshitz transition from a one-dimensional (1D) Fermi surface to a second metal with two Fermi surfaces, made of first 1D and second 2D Fermi surfaces, can be easily reproduced by considering a 1D periodic potential barrier that confines the itinerant charges in 1D wires.

We consider a two-dimensional (2D) super-lattice of quantum stripes in the CuO_2 planes of the cuprate superconductors made of stripes (U) with a finite 1D periodic potential barrier due to stripes (D). The one electron potential looks like barriers of width W, height V_b, and wells of width L in the y direction with periodicity $\lambda_p = L + W$ and is constant along the x direction; it is expressed as

$$V(y) = -V_b \sum_{m=-\infty}^{\infty} \theta\left(\frac{W}{2} - |m\lambda_p - y|\right) \tag{1}$$

The electron effective mass is m^*. The wave functions and the electronic band structure are calculated solving the eigenvalue Schrödinger equation.

$$\begin{aligned} &-\frac{\hbar^2}{2m^*}\nabla^2\psi(x,y) + V(y)\psi(x,y) = E\psi(x,y) \\ &\psi_{n,kx,ky}(x,y) = e^{ikx}\psi_{n,ky}(y) \end{aligned} \tag{2}$$

The eigenvalues are labeled by three quantum number $E = \varepsilon_n(k_x, k_y)$ where n is the subband index, k_x and k_y are the electron wave vector in the 2D superlattice.

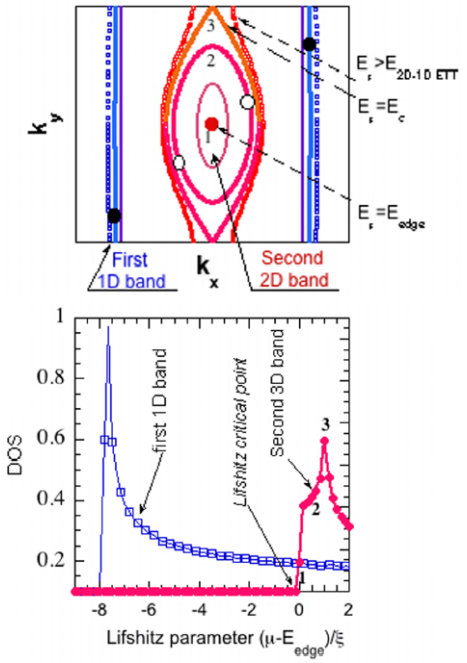

Fig. 2 *Lower panel:* The partial DOS of the first 1D subband (*open squares*, *blue color on line*) and of the second 2D subband (*filled dots*, *red color on line*) as a function of the Lifshitz energy parameter. *Upper panel:* the effect of 2.5 Lifshitz transition on the Fermi surface showing the evolution of the electron-circular Fermi surface at the point of the chemical potential 1,2,3 indicated in the lower panel

Let us assume that below doping $\delta = 1/8$ the chemical potential is tuned below the second subband so that the Fermi surface shown in Fig. 1 is made of open weakly corrugated open lines (blue lines). This regime simulate the 1D metal in the doping range $1/16 < \delta < 1/8$ with a DOS typical of a 1D metal.

The appearing of a second circular electron like Fermi surface at $\delta = 1/18$ is simulated assuming a finite potential barrier. In fact increasing the chemical potential μ we reach the "*2.5 Lifshitz transition*" at the bottom of the second band where $\mu = E_{\text{edge}}$. At this critical point, a new 2D closed circular electron-like Fermi surfaces appears as indicated by the red spots in Fig. 1. The DOS as function of μ shows a jump at E_{edge} as shown in Fig. 2. This critical point simulates the experimental 2.5 *Lifshitz transition* observed in the quantum oscillation experiments [1, 2] at doping $\delta = \text{P}_\text{L} = 1/8$.

This approach provides a model for the evolution of the Fermi surface (FS) topology in the range $1/8 < \delta < 3/16$. In fact, for $\mu > E_{\text{edge}}$ the DOS increases with the chemical potential and the radius of the Fermi surface increases. At this point, there is second topological critical point where the second closed FS open up and form a second 1D Fermi surface called the 2D–1D electronic topological transition (ETT).

For further doping $3/16 < \delta < 4/16$, the system is far from the Mott phase and it can be modeled by a decreasing potential barrier amplitude with increasing doping so that for $\delta = 4/16$ (P*), the Fermi surface becomes a large 2D Fermi surface with a zero potential barriers for the superlattice of stripes.

We consider the presence of an attractive electron-electron (e–e) effective interaction giving Cooper pairs within each Fermi surface involving an energy region ω_0 around the Fermi level

$$V_{nn'}(k,k') = -V u_{nn'}(k_y,k'_y)\vartheta\left(\omega_0 - \left|\varepsilon_n(k) - \varepsilon_\text{F}\right|\right) \times \vartheta\left(\omega_0 - \left|\varepsilon_{n'}(k') - \varepsilon_\text{F}\right|\right) \tag{3}$$

where the function $u_{nn'}(k_y,k'_y)$ is the overlapping integral between the electron pair wave function, $V_{nn'}(k,k')$ is the strength of the interaction and $k = (k_x,k_y)$.

Within the BCS theory, we evaluate the critical temperature T_c numerically solving the BCS multigap equation

$$\Delta_n(k) = -\frac{1}{N_{n'k'}} V_{nn'}(k,k') \frac{\text{tgh}(\frac{\xi_n(k')}{2T_\text{c}})}{2\xi_{n'}(k')} \Delta_{n'}(k') \tag{4}$$

where $\xi_n(k) = \varepsilon_n(k) - \varepsilon_\text{F}$. The isotope exponent is defined as $\alpha = -\partial \ln T_\text{c}/\partial \ln M$ and assuming that the cut-off energy for the interaction is connected with the isotopic mass by $\omega_0 \propto M^{-1/2}$. Therefore, we can write $\alpha = 1/2(\partial \ln T_\text{c}/\partial \ln \omega_0)$ assuming a phonon pairing.

3 The Isotope Effect at the 2.5 Lifshitz Transition

The isotope effect in multigap superconductivity has been recently discussed [44] and it has been shown that it can show large deviations from the standard one-band superconductivity. While in previous studies the assumption of a Fermi level far from a band edge was taken, here we provide the calculation of the isotope effect in a multi-band superconductor near a band edge.

To solve the problem, we start from the solution of the Schrödinger equation, for the 1D periodic potential barrier to obtain the wave-function of the electrons with a free-electron band dispersion along the lattice stripe direction and tight-binding sub-bands in the transversal direction.

The electron density of states (DOS) as a function of the chemical potential shows portions with the 1D power law $1/(E - E_n)1/2$ behavior well above the band edge each subband of the superlattice where the electron wave function is one dimensional. In the energy range between each band edge and the 2D-1D ETT 1D, the electron wave-function has a 2D character as shown in Fig. 2.

We compute the critical temperature T_c of the superconductive transition solving by iteration the BCS equation

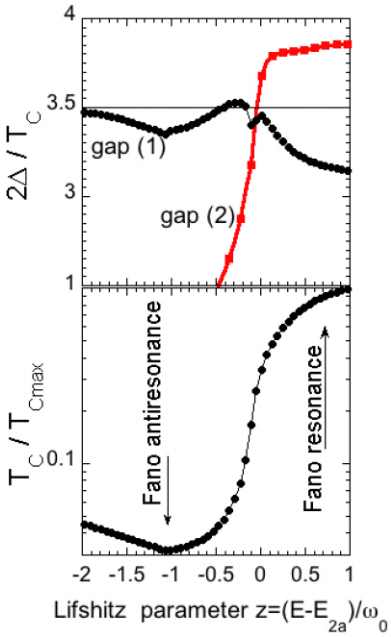

Fig. 3 *Lower panel:* The superconducting critical temperature as a function of the Lifshitz energy parameter showing the minimum at $z = -1$ due to negative interference effect in the Fano resonance called antiresonance; *Upper panel:* the gap ratio $2\Delta/T_c$ for the gap in the first subband (gap(1)) and in the second subband (gap(2))

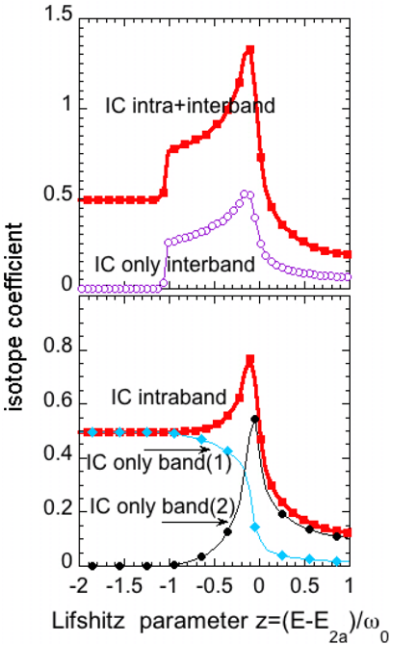

Fig. 4 The isotope coefficient (α) as a function of Lifshitz energy parameter z with the isotope effect (I.E.) acting differently in the intraband Cooper-pairing and in the "interband pairing" Josephson-like channels. *Lower panel:* the variation of α as a function of Lifshitz parameter when the isotope effect is in action only in the intraband 1 (*diamonds*, blue color online) or intraband 2 (*dots*, black color online) channels and for both intraband pairing (*filled squares*, red color online). *Upper panel:* the behavior of α when the I.E. is acting only on the interband paring (*open dots*, violet color online) and when the isotope effect is present in all channels (*filed squares*, red color online)

(4) until a convergence fixed at 10^{-6}, starting with a trial temperature T_1 and finding the T_c by the Newton tangent method. We obtain the T_c for different values of the bulk coupling, defined as $\lambda = N_{n\to\infty}(\varepsilon_F)\ V$ where $N_{n\to\infty}(\varepsilon_F)$ is the DOS of a 2D free electron gas and the values for λ are chosen in the weak—intermediate coupling region ($\lambda = 1/3$). The T_c is evaluated as a function of the chemical potential μ in the proximity in the edge of the 2nd subband. We obtain minimum T_c when μ is approaching the 2.5 Lifshitz transition for the appearance of the 2nd subband as shown in Fig. 3.

In this work, we focus on the antiresonance effect that suppresses the critical temperature at the Lifshitz critical point for the appearing of the second circular Fermi surface. This negative interference effect in the pair transfer between the two condensates produces a minimum in the superconducting critical temperature that we call Fano antiresonance. We assign the experimental decrease of T_c at $P_L = 1/8$ in cuprates to the 2.5 Lifshitz transition at $z = 0$. The calculation indicates also a relevant different gap ratio from the standard value $2\Delta/T_c = 3.5$ for the single band BCS theory with the chemical potential far away from the band edge as shown in Fig. 3.

In Fig. 4, we report the calculated isotope exponent $\alpha(z)$. We show the results of the calculations using experimental constraints on the nature of pairing interaction in the intraband Cooper paring and in the "pair transfer" "Josephson-like" term, called also "interband pairing" channel.

Figure 4 shows that the calculated isotopic exponent $\alpha(z)$, as a function of the Lifshitz parameter z that strongly deviates from the standard BCS value $\alpha_{BCS} = 0.5$ approaching the 2.5 Lifshitz transition while the isotope coefficient is nearly 0.5 far away from the band edge. The Shape resonance in the superconducting gaps that is a type of Fano resonance occurs at $|E - E_{2a}| < \omega_0$ (where E is the chemical potential and E_{2a} the bottom edge of the second band), i.e., at $z = 0$ where we find large deviations of $\alpha(z)$ from 0.5. The isotope coefficient (IC) is 0.5 for $z < 0$ and decreases at $z = 0$ when the isotope effect is present only in the first intraband pairing interaction. At the resonance, there is a smooth decrease at $E - E_{2a} = \omega_0$ and if the isotope effect is in action only in the second subband but not in the first one, the IC shows a smooth increase with threshold at $z = 0$.

Therefore, in the case where the IE is in action in both intraband pairing channels, but not in the exchange like "Josephson-like" "interband pairing" we obtain the maximum of the isotope coefficient at $z = 0$. Therefore, at the 2.5 Lifshitz transition for the appearance of the second circular Fermi surface, i.e., at the band edge of the second subband $E - E_{2a} = \omega_0$ we find a maximum of the isotope coefficient.

These results allow us to understand if the I.E. is acting in specific pairing channels in multicondensate superconduc-

tors by looking to experimental isotope exponent α data for different doping values. This information is very important in order to identify the interplay of phononic or electronic pairing channels in different Fermi surface spots.

4 Conclusions

Starting from a model of structural striped matter made of a superlattice of metallic quantum stripes, we have studied the behavior of the critical temperature T_c and the isotope effect α of the superconducting phase as a function of the chemical potential near the 2.5 Lifshitz transition. When the chemical potential μ is tuned near the 2.5 Lifshitz transition, we find relevant deviations of the isotope exponent $\alpha(z)$ that strongly dependent on the pairing channel where the I.E. is in action.

We have provided a simple model that reproduces the maximum of $\alpha(z)$ and suppression of T_c at P_L where a new electron-like small electron pocket appears in cuprates and a similar scenario is possible in electron doped iron based superconductors [50].

References

1. Laliberte, F., Chang, J., Doiron-Leyraud, N., Hassinger, E., Daou, R., Rondeau, M., Ramshaw, B.J., Liang, R., Bonn, D.A., Hardy, W.N., Pyon, S., Takayama, T., Takagi, H., Sheikin, I., Malone, L., Proust, C., Behnia, K., Taillefer, L.: Nat. Commun. **2**, 432 (2011)
2. LeBoeuf, D., et al.: Phys. Rev. B **83**, 054506 (2011)
3. Doiron-Leyraud, N., et al.: Nature **447**, 565–568 (2007). doi:10.1038/nature05872
4. Sebastian, S.E., Harrison, N., Palm, E., Murphy, T.P., Mielke, C.H., Liang, R., Bonn, D.A., Hardy, W.N., Lonzarich, G.G.: Nature **454**, 200 (2008). ISSN 0028-0836. doi:10.1038/nature07095
5. Singleton, J., et al.: Phys. Rev. Lett. **104**, 086403 (2010). doi:10.1103/PhysRevLett.104.086403
6. Khasanov, R., Strassler, S., Di Castro, D., Masui, T., Miyasaka, S., Tajima, S., Holder, A.B., Keller, H.: Phys. Rev. Lett. **99**, 237601 (2007). doi:10.1103/PhysRevLett.99.237601
7. Boyer, M.C., Wise, W.D., Chatterjee, K., Yi, M., Kondo, T., Takeuchi, T., Ikuta, H., Hudson, E.W.: Nat. Phys. **3**, 802 (2007). doi:10.1038/nphys725
8. Chubukov, A.: Physics **3**, 54 (2010). doi:10.1103/Physics.3.54
9. Norman, M.: Physics **3**, 86 (2010). doi:10.1103/Physics.3.86
10. Ovchinnikov, S.G., Korshunov, M.M., Shneyder, E.I.: J. Exp. Theor. Phys. **109**(5), 775–785 (2009). doi:10.1134/S1063776109110077
11. Norman, M.R., Lin, J., Millis, A.J.: Phys. Rev. B **81**, 180513 (2010)
12. Bianconi, A., De Santis, M., Di Cicco, A., Flank, A.M., Fontaine, A., Lagarde, P., Yoshida, H.K., Kotani, A., Marcelli, A.: Phys. Rev. B **38**, 7196 (1988)
13. Bianconi, A.: Solid State Commun. **89**, 933 (1994)
14. Bianconi, A., Saini, N.L., Rossetti, T., Lanzara, A., Perali, A., Missori, M.: Phys. Rev. B **54**, 12018–12021 (1996)
15. Kugel, K.I., Rakhmanov, A.L., Sboychakov, A.O., Poccia, N., Bianconi, A.: Phys. Rev. B **78**, 165124 (2008). doi:10.1103/PhysRevB.78.165124
16. Kristoffel, N., Rubin, P., Örd, T.: J. Supercond. Nov. Magn. **20**, 571 (2007). ISSN 1557-1939. doi:10.1007/s10948-007-0266-z
17. Bussmann-Holder, A., Bianconi, A.: Phys. Rev. B **67**, 132509 (2003). doi:10.1103/PhysRevB.67.132509
18. Bianconi, A., Bachrach, R.Z.: Phys. Rev. Lett. **42**, 104 (1979)
19. Stizza, S., Mancini, G., Benfatto, M., Natoli, C.R., Garcia, J.: Phys. Rev. B **40**, 12229 (1989)
20. Garcia, J., Bianconi, A., Benfatto, M., Natoli, C.R.: J. Phys., Colloq. **47**, 8 (1986)
21. Garcia, J., Benfatto, M., Natoli, C.R., Bianconi, A., Fontaine, A., Tolentino, H.: Chem. Phys. **132**, 295 (1989)
22. Bianconi, A., Della Longa, S., Missori, M., Pettiti, I., Pompa, M.: In: Bar-Yam, Y., Egami, T., Leon, J.M.-d., Bishop, A.R. (eds.) Lattice Effects in High-T_c Superconductors, pp. 65–76. World Scientific, Singapore (1992)
23. Bianconi, A., Missori, M.: J. Phys. I **4**, 361 (1994)
24. Bianconi, A., Saini, N.L., Lanzara, A., Missori, M., Rossetti, T., Oyanagi, H., Yamaguchi, H., Oka, K., Ito, T.: Phys. Rev. Lett. **76**, 3412 (1996)
25. Bianconi, A., Lusignoli, M., Saini, N.L., Bordet, P., Kvick, Å., Radaelli, P.G.: Phys. Rev. B **54**, 4310 (1996)
26. Bianconi, A., Di Castro, D., Bianconi, G., et al.: Physica C **341**, 1719–1722 (2000). doi:10.1016/S0921-4534(00)00950-3. International Conference on Materials and Mechanisms of Superconductivity High Temperature Superconductors VI, Houston, Texas, 20–25 Feb. 2000
27. Bianconi, A., Saini, N.L., Agrestini, S., Di Castro, D., Bianconi, G.: Int. J. Mod. Phys. B **14**, 3342–3355 (2000)
28. Fratini, M., Poccia, N., Ricci, A., Campi, G., Burghammer, M., Aeppli, G., Bianconi, A.: Nature **466**, 841–844 (2010). doi:10.1038/nature0926
29. Poccia, N., Fratini, M., Ricci, A., Campi, G., Barba, L., Vittorini-Orgeas, A., Bianconi, G., Aeppli, G., Bianconi, A.: Nat. Mater. **10**, 733 (2011). doi:10.1038/nmat3088
30. Poccia, N., Ricci, A., Campi, G., Fratini, M., Puri, A., Di Gioacchino, D., Marcelli, A., Reynolds, M., Burghammer, M., Saini, N.L., Aeppli, G., Bianconi, A.: Proc. Natl. Acad. Sci. USA **109**, 15685 (2012). doi:10.1073/pnas.1208492109
31. Bianconi, A., Agrestini, S., Bianconi, G., et al.: In: Bianconi, A., Saini, N.L. (eds.) Stripes and Related Phenomena, Selected Topics in Superconductivity, pp. 9–25. Kluwer Academic/Plenum Publishers, Dordrecht, New York (2000). Conferente prooceeding of the 2nd International Conference on Stripes and High T_c Superconductivity, Rome, Italy, 02–06 Jun. 1998. http://www.worldcat.org/isbn/9780306464195
32. Bianconi, A., Missori, M., Oyanagi, H., Yamaguchi, H., Ha, D.H., Nishiara, Y., Della Longa, S.: Europhys. Lett. **31**, 411 (1995)
33. Poccia, N., Campi, G., Fratini, M., Ricci, A., Saini, N.L., Bianconi, A.: Phys. Rev. B **84**, 100504 (2011). doi:10.1103/PhysRevB.84.100504
34. Campi, G., Cappelluti, E., Proffen, T., Qiu, X., Bozin Billinge, E.S., Agrestini, S., Saini, N.L., Bianconi, A.: Eur. Phys. J. B, Condens. Matter Complex Syst. **52**, 15 (2006)
35. Saini, N.L., Oyanagi, H., Ito, T., Scagnoli, V., Filippi, M., Agrestini, S., Campi, G., Oka, K., Bianconi, A.: Eur. Phys. J. B, Condens. Matter Complex Syst. **36**, 75 (2003)
36. Bianconi, A.: Solid State Commun. **91**, 1 (1994)
37. Bianconi, A., Missori, M.: Solid State Commun. **91**, 287 (1994)
38. Innocenti, D., Ricci, A., Poccia, N., Campi, G., Fratini, M., Bianconi, A.: J. Supercond. Nov. Magn. **22**, 529–533 (2009)
39. Bianconi, G.: Phys. Rev. E **85**, 061113 (2012)
40. Bianconi, G.: J. Statist. Mech. Theory Exp. **2012**, P07021 (2012)
41. Crawford, M.K., Kunchur, M.N., Farneth, W.E., McCarron, E.M., Poon, S.J.: Phys. Rev. B **41**, 282 (1990). doi:10.1103/PhysRevB.41.282

42. Crawford, M.K., Farneth, W.E., McCarronn, E.M., Harlow, R.L., Moudden, A.H.: Science **250**, 1390 (1990). doi:10.1126/science.250.4986.1390
43. Zhao, G.-M., Hunt, M.B., Keller, H., Muller, K.A.: Nature **385**, 236 (1997). doi:10.1038/385236a0
44. Khasanov, R., Shengelaya, A., Di Castro, D., Morenzoni, E., Maisuradze, A., Savić, I.M., Conder, K., Pomjakushina, E., Holder, A.B., Keller, H.: Phys. Rev. Lett. **101**, 077001 (2008). doi:10.1103/PhysRevLett.101.077001
45. Zech, D., Keller, H., Conder, K., Kaldis, E., Liarokapis, E., Poulakis, N., Muller, K.A.: Nature **371**, 681 (1994). doi:10.1038/371681a0
46. Bussmann-Holder, A., Keller, H., Khasanov, R., Simon, A., Bianconi, A., Bishop, A.R.: New J. Phys. **13**, 093009 (2011). doi:10.1088/1367-2630/13/9/093009
47. Perali, A., Bianconi, A., Lanzara, A., Saini, N.L.: Solid State Commun. **100**, 181 (1996)
48. Bianconi, A., Valletta, A., Perali, A., Saini, N.L.: Solid State Commun. **102**, 369–374 (1997). doi:10.1016/S0038-1098(97)00011
49. Innocenti, D., Poccia, N., Ricci, A., Valletta, A., Caprara, S., Perali, A., Bianconi, A.: Phys. Rev. B **82**, 184528 (2010). doi:10.1103/PhysRevB.82.184528
50. Innocenti, D., Caprara, S., Poccia, N., Ricci, A., Valletta, A., Bianconi, A.: Supercond. Sci. Technol. **24**, 015012 (2011). doi:10.1088/0953-2048/24/1/015012
51. Innocenti, D., Valletta, A., Bianconi, A.: J. Supercond. Nov. Magn. **24**, 31137–31143 (2010). doi:10.1007/s10948-010-1096-y
52. Kresin, V.Z., Bill, A., Wolf, S.A., Ovchinnikov, Yu.N.: Phys. Rev. B **56**, 107 (1997). doi:10.1103/PhysRevB.56.107
53. Kresin, V.Z., Wolf, S.A.: Phys. Rev. B **49**, 3652 (1994). doi:10.1103/PhysRevB.49.3652